CMLS, Cell. Mol. Life Sci. 60 (2003) 979–990
1420-682X/03/050979-12
DOI 10.1007/s00018-003-2365-x

CMLS Cellular and Molecular Life Sciences

Research Article

Chromosomal territory segmentation in apoptotic cells

E. Bártová, P. Jirsová, M. Fojtová, K. Souček and S. Kozubek*

Institute of Biophysics, Academy of Sciences of the Czech Republic, Královopolská 135, 612 65 Brno (Czech Republic), Fax + 4205 41240498, e-mail: kozubek@ibp.cz

Received 18 December 2002; received after revision 17 February 2003; accepted 4 March 2003

Abstract. The nuclear architecture of selected chromosomes in apoptotic nuclei of human leukemic cells K-562 and HL-60 was investigated. Etoposide and prolonged confluence were used for the induction of apoptosis. DAPI as well as TUNEL labeling of apoptotic nuclear bodies was combined with visualization of chromosomal territories by the FISH technique. Simultaneous vital staining by annexin V, propidium iodide, and Hoechst 33342 was applied to distinguish apoptotic, necrotic, and intact cell fraction of tested populations. Our FISH analyses revealed that the three-dimensional (3D) structure of apoptotic nuclei as well as the 3D structure of apoptotic bodies is preserved in formaldehyde-fixed cells. High-molecular-weight DNA fragmentation was determined in apoptotic K-562 cells in contrast to oligonucleosomal cleavage observed in apoptotic HL-60 cells. In K-562 populations, chromosomal territories were located separately either in one apoptotic body or underwent disassembly into chromosomal segments dispersed into single and/or several apoptotic bodies. The apoptotic disorganization of chromosomal territories was irregular, leading mainly to chromosomal segments of different sizes and, consequently, chromosomal disassembly was not observed at specific sites. In comparison with the control, an increased number of centromeric FISH signals were observed in prolonged confluence-treated K-562 cells induced to apoptosis. This finding can be explained either as a consequence of apoptosis or by polyploidization. Sequential staining of the same apoptotic nuclei by the FISH and TUNEL techniques revealed that chromosomal territory segmentation precedes the formation of nuclear apoptotic bodies.

Key words. Chromosomal territory; nuclear architecture; apoptosis; DNA fragmentation.

Apoptosis is an active cell death defined by many morphological and biochemical events resulting in physiological cell loss from an organism. This biological process is completely different from the pathophysiological cell state called necrosis, which induces inflammatory responses. Cell shrinkage, nuclear condensation, DNA degradation into specific DNA fragments, membrane blebbing, and the formation of small cell bodies surrounded by intact cell membranes are typical features of apoptosis [1, 2]. In contrast to necrosis, apoptotic cells do not swell, and apoptotic particles undergo phagocytosis before losing their intracellular content [3, 4].

* Corresponding author.

Most of the visible morphological and structural aspects characterizing apoptotic cell death are ascribed to the activation of a unique family of cysteine proteases called caspases [5, 6]. These enzymes can be considered as central regulators of the apoptotic machinery [7]. A caspase-activated DNase called CAD (DNA ladder nuclease) preexists in living cells with an inhibitory subunit ICAD. Caspase-3 mediates cleavage of ICAD, which leads to CAD activation [7]. This process is responsible for DNA fragmentation, one of the specific events observed in an apoptotic nucleus. The mechanisms that induce nuclear changes typical of apoptosis have been only partially clarified [7–10]. Three types of DNA fragmentation have been described. The first involves cleavage of the genome

into large fragments of about 50–300 kbp [8, 11] and/or 50–700 kbp [12]. This type of fragmentation has been referred as 'domain' cleavage, which correlates with the chromatin relocation outward against the nuclear periphery [8]. This process is mediated by topoisomerase II activation [13, 14]. The second type of DNA fragmentation is oligonucleosomal laddering which involves 180- to 200-bp lengths. Activation of the nucleases responsible for nucleosomal fragmentation is considered to be one of the most important pro-apoptotic phenomena [15]. The third possibility is the formation of single-stranded DNA breaks [9]. Several observations indicate that all types of apoptosis are accompanied by DNA fragmentation into large 50- to 300-kbp segments [summarized in ref. 8], which are further degraded to smaller units of 10–40 kbp [16] but not all cell lines undergo final oligonucleosomal fragmentation [summarized in ref. 10], which is carried out by DNase I and DNase II cleavage of chromosomal DNA at linker regions [17]. On the other hand, direct cleavage of apoptotic DNA into 180- to 200-bp fragments was described by Bortner et al. [9].

Apoptosis is a gene-directed process connected with two major apoptotic pathways. The death receptor pathway involves the binding of the death receptor superfamily member CD95 (Apo-1/Fas) to the CD95 ligand. This complex recruits via the adaptor molecule FADD and procaspase-8 molecules are initiated, which leads to caspase-8 activation. The next important pro-apoptotic pathway is mediated via mitochondria and is used in response to extracellular signals and internal insults such as DNA damage. In this pathway, pro-apoptotic members of the Bcl-2 family, associated with the mitochondrial surface, are activated, inducing the exit of cytochrome c from mitochondria. Cytochrome c associates with Apaf 1 and procaspase-9 to form the apoptosome [summarized in ref. 7]. Both death receptor and mitochondrial pathways converge at the level of caspase-3 activation, which is responsible for cleavage of substrates mentioned above mediating the process of apoptosis [7]. Activation of various signaling apoptotic pathways transfers signals from outside the cells into the cytosol and subsequently into the nuclear interior. These processes also induce activation of specific genes playing an important role during induction of apoptosis. The tumor suppressor gene p53 and proto-oncogene c-myc have been shown to be related to the apoptotic machinery [18, 19]. p53-dependent cell deaths converge on cytochrome c release from the mitochondria and subsequent caspase activation [20, 21]. Several pro-apoptotic activities have also been suggested for the non-receptor tyrosine kinase gene Abl, whose function during apoptosis has only been partially clarified [summarized in ref. 22].

This article is concerned with the relationship between the terminal apoptotic programmed cell death and the architecture of chromosomal territories. Chromosomes are organized into distinct territories within the interphase nucleus [23–27]. The mammalian genome undergoes many DNA modifications, which are related to specific changes in nuclear architecture observed not only during DNA repair, but also during replication, transcription and splicing [summarized in ref. 25]. Certain cellular processes, such as terminal differentiation, are also accompanied by higher-order chromatin structure modifications [28–31]. In cell nuclei, chromosomal territories and the interchromatin compartment [23–25] can be distinguished. These structures are largely conserved during nuclear and cellular processes.

During apoptosis, chromatin collapses against the nuclear periphery, becomes more condensed, the final level of condensation being dramatic and the nucleus seen as an assemblage of nuclear apoptotic bodies [8]. However, there is a lack of evidence related to the organization of chromosomal territories in apoptotic nuclei.

Materials and methods

Cell cultivation and induction of apoptosis

K-562 (ECACC No. 89121407), the human leukemic cell line, was obtained from the European Collection of Cell Cultures (ECACC). The cells were cultivated in RPMI-1640 medium, supplemented with 10% fetal calf serum (PAN, Biotech, Aidenbach, Germany), at 37°C in a humidified atmosphere containing 5% CO_2. HL-60 leukemic cells (ATTC No. CCL-240) were obtained from the American Tissue Culture Collection (ATCC) and were cultivated in IMDM medium supplemented with 10% fetal calf serum. Apoptosis was induced in HL-60 and K-562 cells by prolonged confluence (cultivation for 8 days without medium change) and using etoposide (20 μM for 72 h).

Three-dimensional cell fixation and permeabilization

Cytological preparations were made utilizing cell fixation by paraformaldehyde. The cells were fixed in 4% formaldehyde in PBS for 5 min, washed thoroughly in PBS (3 × 4 min), permeabilized for 10 min in 0.2% saponine dissolved in PBS, followed by treatment with 0.2% Triton X-100 in PBS for 10 min. Fixed cells were washed in 0.1 M Tris-HCl (pH 7.2) for 15 min and equilibrated in 20% glycerol in PBS for 20 min. Freezing the slides in liquid nitrogen was the following step. Before hybridization, the target DNA was denatured in 50% formamide in 2 × SSC for 15 min at 80°C [32]. Long-term denaturation was necessary for chromosomal DNA probe penetration into the formaldehyde-fixed apoptotic bodies of tested cells.

Fluorescence in situ hybridization in three dimensionally preserved apoptotic bodies

Digoxigenin- and biotinyl-labeled DNA probes were obtained from Oncor (Gaithersburg, Md.) and Cambio

(Cambridge, UK). We studied territories of chromosomes 11, 17, 21, and alpha-satellite sequences of chromosome 11. The conditions for the hybridization and post-hybridization wash were selected according to the instructions of the manufacturer and in accordance with Bártová et al. [30, 31].

Image acquisition

A high-resolution cytometer Zeiss Axiovert 100 microscope (Zeiss, Jena, Germany) equipped with a confocal Carv unit (Atto Instruments, New York, N. Y.) was used for image acquisition. The images (40 optical sections with an axial step of 0.3 μm) were captured with a fully programmable digital CCD Micromax camera (Princeton Instruments, Princeton, N. J.). The cytometer was computer controlled, acquisition was performed using FISH 2.0 software [33]. In the case of apoptotic cells, about 500 images obtained from the 40 optical sections (axial step 0.3 μm) were stored in the computer memory and analyzed. A laser scanning system (QLC100; Visi-Tech International, Sunderland, U. K.) connected to a Leica DM-RXA epi-fluorescence microscope was also used to distinguish precise apoptotic morphology.

Flow cytometric analysis of the cell cycle and sub-G1 apoptotic peak determination

Flow cytometric detection of the sub-G1 peak in the cell cycle profile was performed in accordance with Bártová et al. [34]. The cells were fixed in 70% ethanol at –20 °C for 30 min, then washed twice with PBS and stained with 10 μg/ml propidium iodide (PI) in Vindel's solution (1 mM Tris-Cl, pH 8.0, 1 mM NaCl, 0.1% Triton X-100, 10 μg/ml RNase A) at 37 °C for 30 min. The DNA profile was measured with a FACSCalibur flow cytometer (Becton Dickinson, Heidelberg, Germany), using CellQuest 3.0 software. Analysis of the cell cycle phases and cell quantification in the apoptotic sub-G1 peak was done with the aid of the automatic analysis of ModFit software (Verity Software House, Topsham, USA).

Vital staining of apoptotic cells

For precise characterization of apoptotic cell populations, vital staining of apoptotic cells was performed. FITC-conjugated annexin V (Roche Diagnostics, Mannheim, Germany) and PI were used for flow cytometric analysis. Flow cytometric data were evaluated as a percentage of double-negative cells (intact), annexin-V-positive cells (early apoptotic), and double-positive (necrotic or late apoptotic) cells. CellQuest 3.0 software (Becton Dickinson), connected to a FACSCalibur flow cytometer, was used for data analysis. In addition, growing etoposide-treated and control cells were incubated with Hoechst 33342 (1 μg/ml, for 30 min) and PI (10 μg/ml for the last 5 min) to distinguish necrotic and late apoptotic cells according to the specific morphology. After this vital staining, the tested cell populations were analyzed by fluorescence microscopy. To obtain a precise description of apoptotic cell populations we additionally measured the mitochondrial membrane potential ($\Delta\psi_m$) using tetramethylrhodamine ethyl ester perchlorate (TMRE; Molecular Probes, Leiden, The Netherlands). The methodology was in accordance with Vondráček et al. [35].

DNA fragmentation test

DNA isolation was carried out in the following steps: 2×10^7 cells were washed in PBS and then resuspended in lysis buffer (10 mM Tris-HCl, pH 8.0, and 2 mM EDTA) containing 1% SDS. Proteinase K (0.2 mg/ml) was added and overnight incubation at 37 °C followed. RNase was used at a final concentration of 0.25 mg/ml at 37 °C for 2 h. Phenol : chloroform : isoamyl alcohol (25 : 24 : 1) were applied and the final aqueous phase of DNA was mixed with 1/10 vol of 3 M sodium acetate and 2 vol of 100% cold ethanol (–20 °C). After centrifugation and lyophilization, the DNA was dissolved in a TE buffer (10 mM Tris-HCl, pH 8.0, and 1 mM EDTA). Agarose gel electrophoresis (1.8%) was run in 1 × TBE buffer (89 mM Tris-Cl, 89 mM H_3BO_3, 2 mM EDTA, pH 8.0). Ethidium bromide (1 μg/ml) was used for DNA visualization and a DNA marker (pBR322/*Msp*I) for fragment length verification.

Pulse field gel electrophoresis

The cells were washed twice in PBS and resuspended at a density of $8–10 \times 10^6$ with a 50 °C buffer containing 1 mM Tris-Cl, 50 mM EDTA, 0.4 M mannitol (pH 6.0). The same volume of 2% low-melting agarose dissolved in 0.4 M mannitol, 20 mM MES (pH 5.35) at 50 °C was used. The plugs were digested for 48 h at 50 °C with proteinase K (1 mg/ml) dissolved in 0.5 M EDTA with 1% lauroylsarcosine, then washed three times in 0.5 M EDTA and immersed into 0.5 × TBE (45 mM Tris-borate, 1 mM EDTA, pH 8.0). Electrophoresis was carried out using a horizontal gel chamber of the Gene Navigator System (Pharmacia Biotech, Uppsala, Sweden). The running conditions (pulse ramping time from 5 to 50 s, voltage 200 V, temperature 10 °C, time 22 h) enabled separation of fragments between 50–1000 kbp in size. As a running buffer we used 0.5 × TBE. Large concatemers of lambda DNA (48.5–727.5 kbp) were used as a DNA marker. After electrophoresis, the gel was stained with ethidium bromide (1 μg/ml).

TUNEL test

This method involves the separation of fragmented DNA from non-fragmented, high-molecular-weight DNA in a given cell population. The DNA cleavage may yield double-stranded as well as single-stranded DNA breaks (nicks). Both types of break can be detected by labeling the free 3′-OH termini with modified nucleotides (we

used fluorescein-dUTP) in an enzymatic reaction. The enzyme terminal deoxynucleotidyl transferase (TdT) catalyzes the template-independent polymerization of deoxyribonucleotides to the 3′ end of single- and double-stranded DNA. The In Situ Cell Death Detection Kit, Fluorescein (Roche Diagnostics) allows qualitative detection of apoptosis at the single-cell level by fluorescence microscopy. Apoptotic cells were fixed in 4% formaldehyde and washed twice in PBS. Subsequently, the cells were incubated for 60 min at 37 °C in a humidified atmosphere with 50 µl of TUNEL reaction mixture. After washing three times in PBS, TUNEL-positive cells were analyzed by a laser scanning system (QLC100; Visi Tech International) connected to a LeicaDMRXA epi-fluorescence microscope controlled by FISH 2.0 software. Negative as well as positive controls related to the TUNEL test were done according to the instructions of the manufacturer (Roche Diagnostics). Simultaneous additional staining by TUNEL, PI and DAPI was performed to exactly distinguish terminal stages of apoptosis.

Results

Apoptosis and DNA fragmentation

The topoisomerase II inhibitor etoposide and prolonged confluence were used for studies of apoptotic DNA fragmentation in human leukemic K-562 cells. Pulse field gel electrophoresis (PFGE) revealed the presence of large DNA fragments whose length was verified using concatemers of lambda DNA (see fig. 1 A, lane 1). Cleavage into 50 kbp was found after etoposide and prolonged confluence treatment (fig. 1 A, lanes 2, 3). The fragments between 250–300 kbp were visible only in the case of etoposide exposure (fig. 1 A, lane 2). In both tested treatments of K-562 cells, we did not observe an oligonucleosomal DNA ladder (see fig. 1 B, lanes 2′, 3′) that was determined only in the case of prolonged confluence of HL-60 cells (fig. 1 B, lane 4′). Large DNA fragmentation was not detected in prolonged confluence of HL-60 cells (fig. 1 A, lane 4). In our experiments, we analyzed a heterogenous cell population involving a certain percentage of intact as well as apoptotic cells (up to 50% apoptotic nuclei). This resulted in our ability to observe both high-molecular non-fragmented DNA (lane 4) as well as 180–200-bp fragments (lane 4′) in a population of HL-60 cells undergoing prolonged confluence. Oligonucleosomal fragmentation was compared with a DNA marker (pBR322/*Msp*I) (fig. 1 B, lane 1′) and both apoptotic DNA tests were also done in a control K-562 (HL-60) cell population characterized by non-fragmented DNA (see legend to fig. 1 A, B, lanes 5 and 5′).

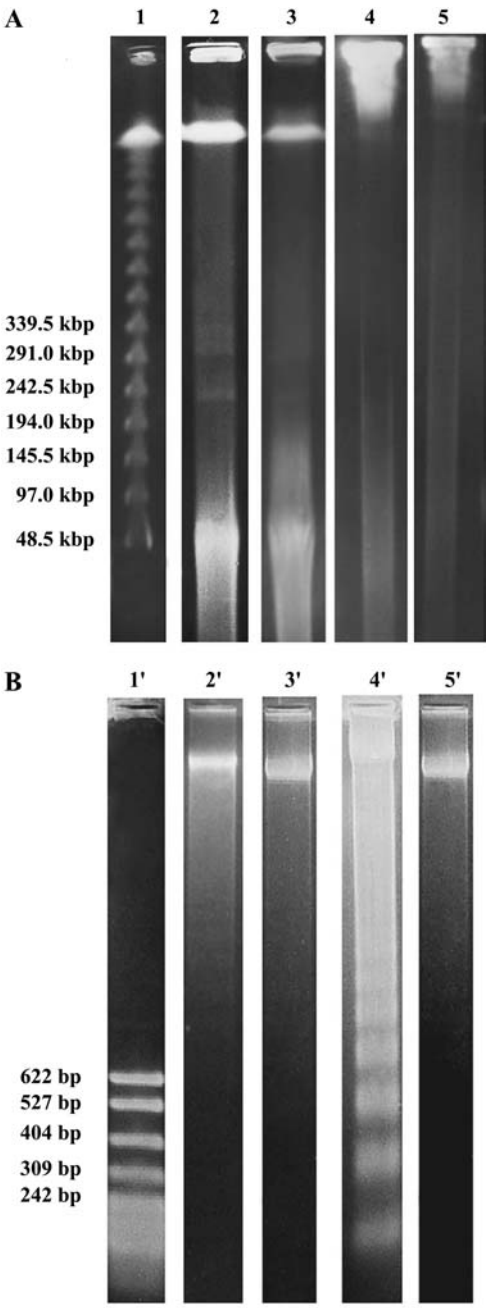

Figure 1. (*A*) Large DNA fragmentation was studied using PFGE. Lane 1, lambda DNA concatemers (48.5–727.5 kbp; lane 2, K-562 cell DNA cleaved into 50 and 300 kbp after cell exposure to etoposide; lane 3, K-562 cell DNA cleaved into 50 kbp after prolonged confluence treatment; lane 4, absence of large DNA fragmentation in HL-60 cells undergoing prolonged confluence; lane 5, non-treated K-562 cells and standard growing HL-60 cells (not shown) were used as a control. (*B*) The presence of oligonucleosomal fragments was determined using a DNA fragmentation test. Lane 1′, DNA marker (pBR322/*Msp*I); lane 2′, oligonucleosomal cleavage was not observed in K-562 cell DNA isolated from etoposide treated cells; lane 3′, absence of oligonucleosomal cleavage in K-562 cells after prolonged confluence treatment; lane 4′, HL-60 cells undergoing prolonged confluence showed the 180- to 200 bp DNA ladder; lane 5′, DNA of K-562 control cells.

Morphological features of apoptosis and results of TUNEL test

Confocal microscopy was used to determine the morphological features of apoptosis. The presence of nuclear apoptotic bodies and chromatin margination were observed after DAPI staining as well as after the TUNEL test in experiments using three-dimensional (3D) confocal microscopy (fig. 2). Non-apoptotic cells were characterized by low fluorescence (autofluorescence), which was due to non-incorporated fluorescein-dUTP (fig. 2A). On the other hand, apoptotic DNA was intensively stained by fluorescein-dUTP used in the TUNEL reaction (fig. 2B). 3D organization of TUNEL-stained DNA in the apoptotic nucleus is shown in x-y, x-z, and y-z projections (fig. 2C–E). Chromatin margination and formation of spatially organized apoptotic bodies, as a general feature of apoptosis, is shown after DAPI staining in figure 2F–I. As can be seen, the formaldehyde fixation largely preserved the 3D structure of apoptotic nuclei as well as the 3D structure of the bodies. Apoptotic bodies of different sizes were observed (fig. 2B).

In our experiments, differences between etoposide and prolonged confluence treatment were found with regard to the percentage of apoptotic cells in the K-562 population (fig. 3A). In addition, we observed a different number of apoptotic nuclear bodies (DAPI stained) after

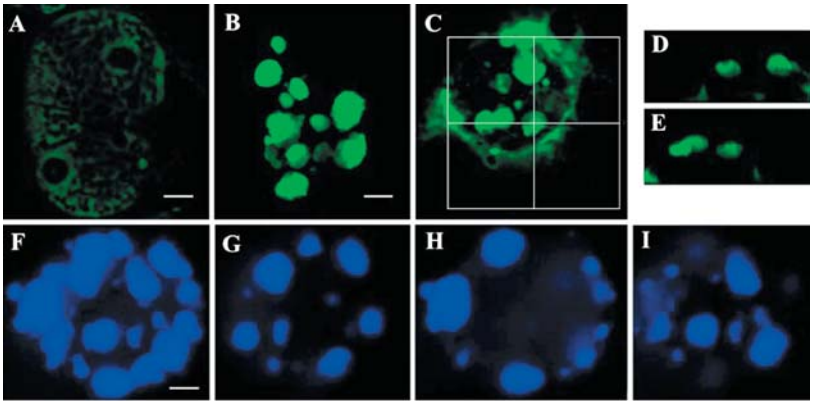

Figure 2. The QLC100 laser scanning system (VisiTech International) connected to a Leica DMRXA epi-fluorescence microscope was used to determine the 3D structure of TUNEL-stained apoptotic nuclei containing nuclear bodies. Bars, 1 µm. (*A*) Autofluorescence of intact interphase nuclei of K-562 cells. (*B*) Intensive incorporation of fluorescein-dUTP into apoptotic nuclear bodies of K-562 cells treated with etoposide. (*C–E*) 3D projections involving x-y (*C*), y-z (*D*), and x-z (*E*) images of an etoposide-treated K-562 cell. (*F–I*) Chromatin margination and spatial organization of DAPI-stained apoptotic nuclear bodies in different optical sections were determined in K-562 cells undergoing etoposide treatment.

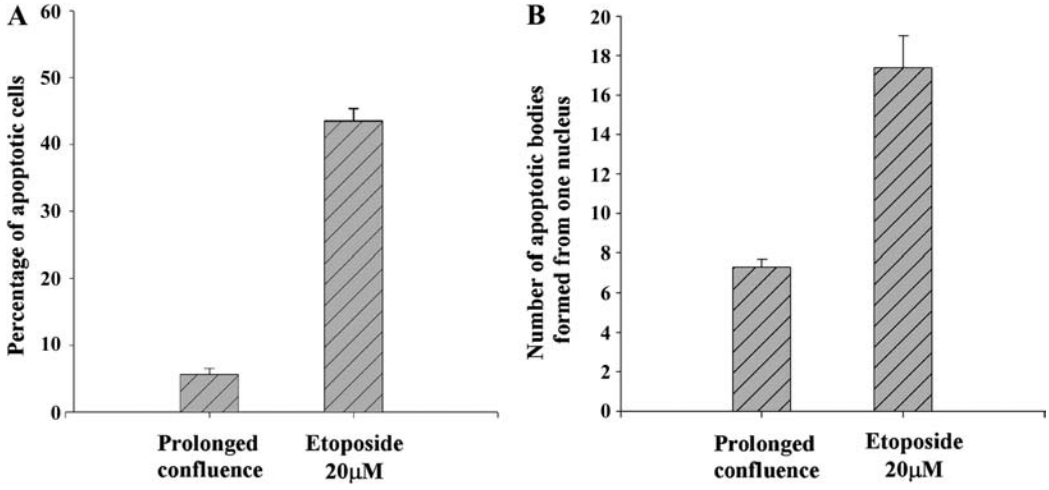

Figure 3. (*A*) Etoposide and prolonged confluence treatments induced a different percentage of apoptotic cells in the K-562 population. (*B*) A substantially larger number of apoptotic nuclear bodies per cell was also found after etoposide as compared to prolonged confluence exposure. After prolonged confluence, more that 2000 nuclei were analyzed to obtain approximately 200 nuclei positive for apoptosis. In the case of etoposide treatment, approximately 500 nuclei were analyzed to obtain 200 nuclei positive for apoptosis. The 200 obtained apoptotic nuclei were further analyzed and the number of apoptotic bodies per nucleus was determined.

etoposide as compared to prolonged confluence exposure (fig. 3B). Etoposide was found to be more effective in apoptotic body formation.

Flow cytometric and morphological detection of apoptotic cells

Flow cytometric DNA analysis was used to determine the presence of the apoptotic sub-G1 peak in our tested cell populations. Control K-562 cells were characterized by a standard non-apoptotic DNA profile (fig. 4A); in the case of prolonged confluence, we found 7.8% of cells in the sub-G1 peak (fig. 4B). The presence of a sub-G1 apoptotic peak was also detected after etoposide treatment (fig. 4C) and ModFit software analysis revealed 26.3% of cells in the sub-G1 phase of the cell cycle.

Terminal stages of apoptotic and necrotic cells could be both characterized by annexin and PI positivity (see fig. 5A, upper right quadrant). Annexin V used in vital staining can bind to phosphatidylserines that are translocated from the inner side of the plasma membrane to the cell surface soon after the induction of apoptosis. On the other hand, necrotic cells could also be positive for such staining. Using flow cytometric analysis of the annexin-V-and PI-stained apoptotic K-562 population (fig. 5A) as well as control K-562 cells (fig. 5B), we showed that there are 24.6% of unambiguously apoptotic cells after etoposide treatment. The cell fraction in the upper right quadrant of the plot in figure 5A (7.1%) could be either the result of secondary necrosis or late apoptosis. Due to this observation, we performed further vital analyses using dual staining with Hoechst 33342 and the viability-determining agent PI. This technique revealed that all cells in the tested population that have a permeabilized cell membrane are not secondarily necrotic cells but represent a terminal stage of apoptosis (fig. 5C) which behaves as necrotic after PI staining. Microscopically the PI-positive cells were verified to show the morphology of late apoptosis (see fig. 5C and compare with control fig. 5D). The total fraction of apoptotic cells, in the etoposide-treated K-562 population, was between 40–50%, as determined microscopically (fig. 3A).

Quantitative measurement of the mitochondrial membrane potential with the aid of TMRE revealed that approximately 41% of cells was in the apoptotic fraction (compare fig. 5E with control fig. 5F). In addition, we also performed dual staining by the TUNEL test and PI on formaldehyde-fixed K-562 cells. We found that nuclei of healthy cells were dimly fluorescent after TUNEL analysis (probably due to autofluorescence) (fig. 6A). Intact nuclei were stained by the DNA-intercalating agent PI as well as the AT-sensitive DAPI (fig. 6B, C). Apoptotic nuclei with apoptotic bodies (final stage of apoptosis) were intensively stained by TUNEL, PI, as well as DAPI (fig. 6D–F). Using a dual fluorescence filter (combination of filters for fluorescein and PI), we found

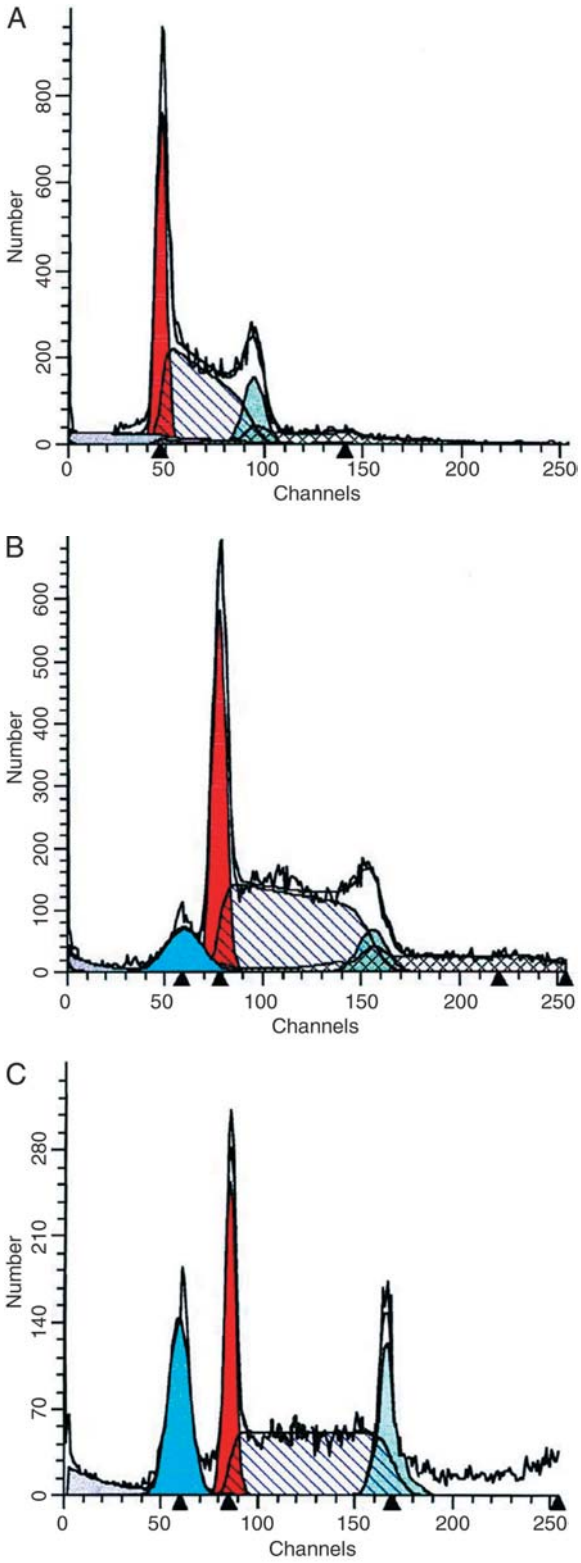

Figure 4. The apoptotic sub-G1 peak was determined using ModFit software analysis of DNA histograms obtained using CellQuest 3.0 software connected to a FACSCalibur flow cytometer. Sub-G1 peak (blue), G1 (red), S (dashed area), G2/M (green). (*A*) DNA analysis of control K-562 cells. (*B*) DNA histogram of K-562 cells undergoing prolonged confluence. (*C*) Cell cycle profile determined after etoposide treatment of K-562 cells.

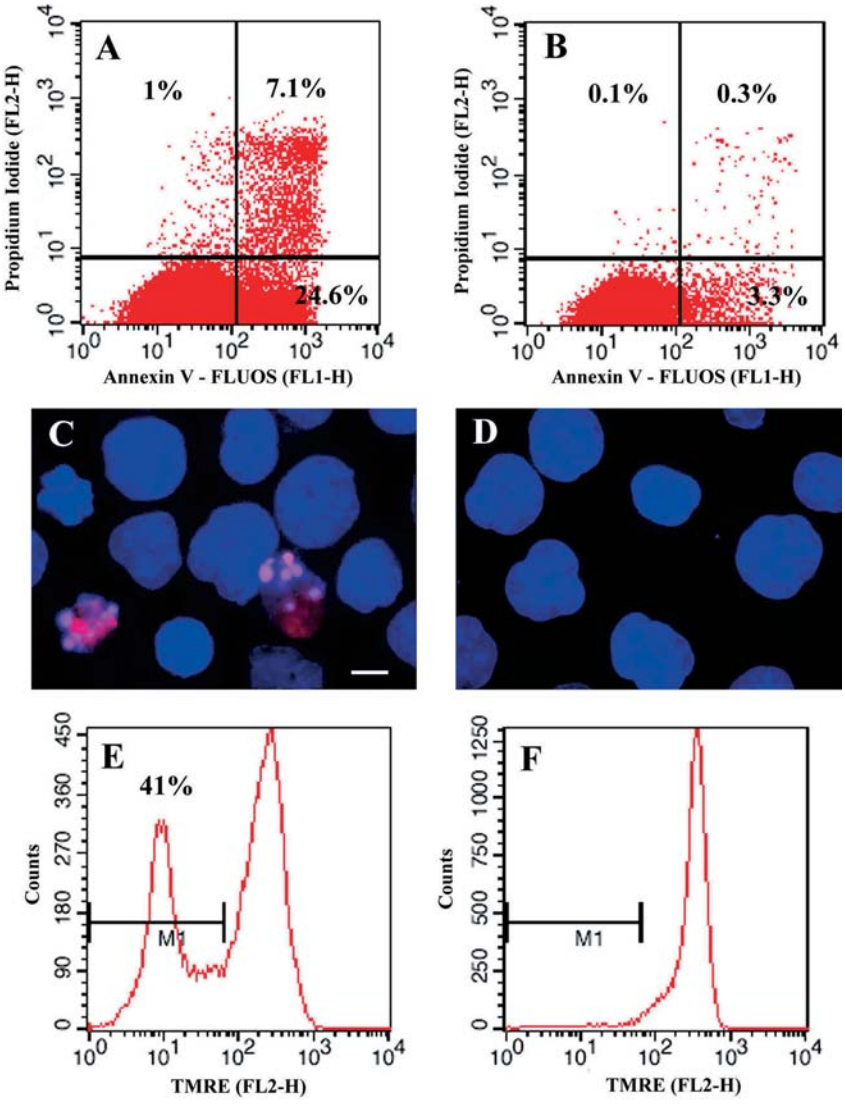

Figure 5. Vital simultaneous staining by annexin V and PI was used to distinguish the intact, apoptotic, and necrotic fraction of K-562 cells treated with etoposide (20 µM, 72 h). Two independent measurements were done using a FACSCalibur flow cytometer. (*A*) 24.6% (21.4% in the second measurement) of cells were found in the apoptotic fraction and 7.1% (10.1% in the second measurement) were observed as secondarily necrotic and/or late apoptotic cells. (*B*) Control K-562 cell population stained by with annexin V and PI showed 0.3% of late apoptotic and/or necrotic cells. (*C*) To distinguish secondary necrosis from terminal stages of apoptosis, simultaneous staining with Hoechst 33342 and PI was performed. All annexin- and PI-positive cells (determined in upper right quadrant of (*A*)) were not secondarily necrotic but late apoptotic (*C*). Bar 2.5 µm. (*D*) Hoechst 33342 and PI staining was also done in control K-562 cells. (*E, F*) For precise verification of the apoptotic cell population, the mitochondrial membrane potential was quantified using TMRE in two independent experiments. (*E*) 41% (26% in the second measurement) of cells were observed in the apoptotic fraction (M1). (*F*) The mitochondrial membrane potential was also studied in control K-562 cells.

that apoptotic nuclei (nuclear bodies) looked yellow (fig. 6G) and healthy intact nuclei were reddish (fig. 6H). In our experiments, we also observed relatively intact nuclei imaged as yellow by dual filter. Morphological analysis showed that these nuclei contain remnants of markedly modified nucleoli (fig. 6I). These nuclei were considered as pre-apoptotic due to a high incorporation of fluorescein-dUTP involved in the TUNEL test and due to their typical morphology.

Apoptosis and chromosomal territories

Territories of chromosomes 11, 17, and 21 were visualized by the fluorescence in situ hybridization (FISH) technique. In erythroleukemia K-562 cells obtained from ECACC, three territories of the studied chromosomes were detected. Studies of apoptotic nuclei provided evidence that (i) segments of FISH-stained chromosomal territories were clearly visible in K-562 apoptotic bodies (fig. 7), but not in leukemic HL-60 cells. (ii) Apoptosis of

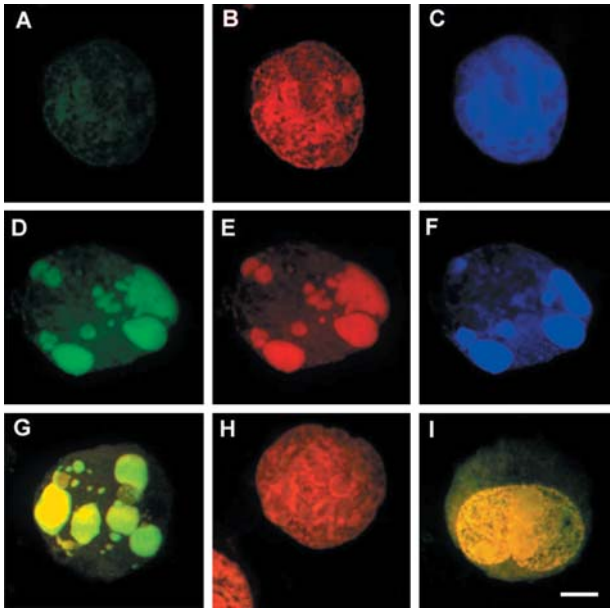

Figure 6. (*A*) Healthy nuclei were dimly fluorescent after TUNEL analysis. (*B*) Healthy nuclei were stained by PI. (*C*) Intact fixed cell nuclei were also DAPI positive. (*D–F*) After etoposide treatment of K-562 cells, fixed apoptotic nuclei with apoptotic bodies (final stage of apoptosis) were intensively stained by TUNEL (*D*), PI (*E*), as well as DAPI (*F*). (*G–I*) After TUNEL and PI staining and using a dual fluorescence filter, we observed that apoptotic nuclei (nuclear bodies) looked yellow (*G*) and healthy intact nuclei were reddish (*H*). Pre-apoptotic stages imaged as yellow by dual filter contained morphologically modified nucleoli (*I*). QLC100 laser scanning system (Visi-Tech International) connected to a Leica DMRXA epi-fluorescence microscope was used for image acquisition. Bar, 2 µm.

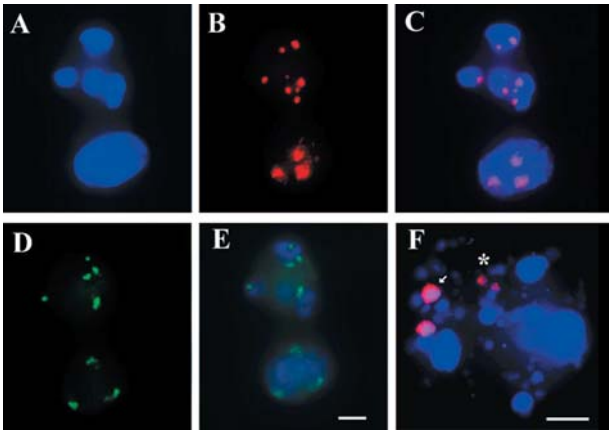

Figure 7. (*A*) DAPI counterstaining was used to visualize of apoptotic bodies in etoposide-treated K-562 cell. The upper cell is apoptotic. (*B*) Chromosome 11 territories (red fluorescence) painted in a apoptotic nucleus of K-562 cell. (*C*) Superposition of images *A* and *B*. (*D*) Chromosome 17 territories (green fluorescence) painted in an apoptotic (upper cell) nucleus of a K-562 cell. (*E*) Superposition of images *A* and *D*. In both cases, three chromosomal copies were found in the interphase nuclei of the control leukemic cell population. Large chromosomal segments of different volume were found in separate apoptotic bodies (*C*, *E*, *F*). Cleaved territories of both studied chromosomes were also observed in the same apoptotic body (mainly *C* and *E*). (*F*) Variable disassembly of chromosome 11 territories is demonstrated: the chromosomal territory was found to be located either in one apoptotic body (arrow) or as large segments disassembled into two neighboring apoptotic nuclear bodies (star). Bar, 2 µm (*E*) or 1 µm (*F*).

K-562 cells was characterized by high-molecular-weight DNA fragmentation (fig. 1A, lanes 2, 3) in contrast to oligonucleosomal fragmentation of HL-60 cells undergoing prolonged confluence (fig. 1B, lane 4′). Moreover, an oligonucleosomal ladder was not observed in the K-562 apoptotic population (fig. 1B, lanes 2′, 3′). Variable disassembly of chromosomal territories was detected in K-562 cells (fig. 7A–F); i.e., some territories were preserved, while others were separated. (iii) Whole territories or large territorial segments were found to be organized in one apoptotic body. In this case, they could be either alone (fig. 7F, arrow) or together with other types of chromosomes (overlay fig. 7C, E). Another form of chromosome disassembly was disassociation into several separated apoptotic bodies (fig. 7F, star). The number of FISH signals (corresponding to chromosomal segments in nuclei of etoposide-treated cells) was 6.8 ± 1.5 which was independent of the number of apoptotic bodies (approximately 17 per etoposide-treated cell).

All our observations lead to the same conclusion regarding variability in apoptotic chromosomal territory disassembly and segregation into apoptotic bodies of the cell types with large-scale (50–300 kbp) DNA fragmentation in their nuclei.

Apoptosis and location of centromeric regions within chromosomal territories

We also studied the spatial position of the alpha-satellite centromeric region of chromosome 11 and the total chromosome 11 territory in the apoptotic bodies of K-562 leukemic cells. Confocal microscopy, used for simultaneous visualization of chromosome 11 territories and their centromeric sequences in 3D-preserved apoptotic cells, revealed variable disassembly of chromosomal territories (fig. 8A) and their centromeric regions (fig. 8B). The overlay image (fig. 8C) shows the location of centromeric regions within the chromosome 11 territory in the apoptotic nucleus of a K-562 cell. For comparison, the nuclear topography of the same chromatin structures is shown in the intact interphase K-562 nucleus (fig. 8D). In these experiments, cell death was induced by prolonged confluence treatment. In some cases, disassociation of the chromosomal territory could be observed in a centromeric region with several centromeric segments visible. On average, six centromeric FISH signals were observed in 30% of the tested apoptotic population, which might be related to apoptosis. On the other hand, Melixetian et al. [36] and Mailhes et al. [37] demon-

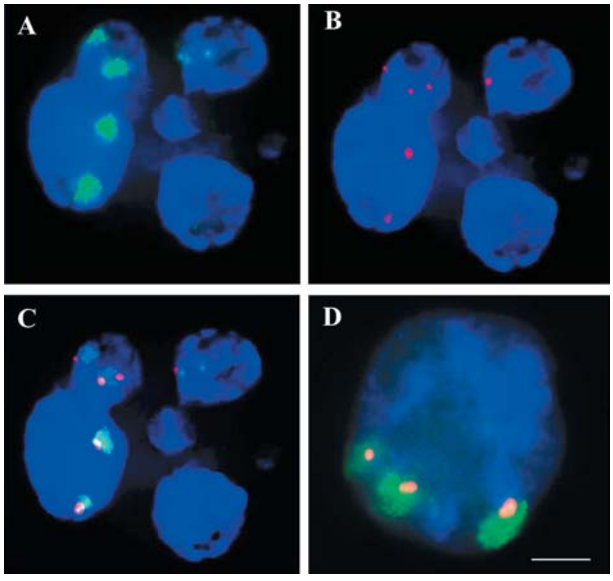

Figure 8. (*A*–*C*) Simultaneous visualization of chromosome 11 territories (green fluorescence) and related centromeric regions (red fluorescence) in K-562 cell induced to apoptosis using prolonged confluence. (*C*) Approximately six centromeric FISH signals were observed in more than 30% of tested apoptotic nuclei, which might be either the consequence of apoptosis or polyploidization. (*D*) The interphase K-562 cell nuclei were typically triploid. Cell nuclei with a higher chromosomal copy number than triploid were found only in 2% of the tested cell population. Bar, 0.7 µm.

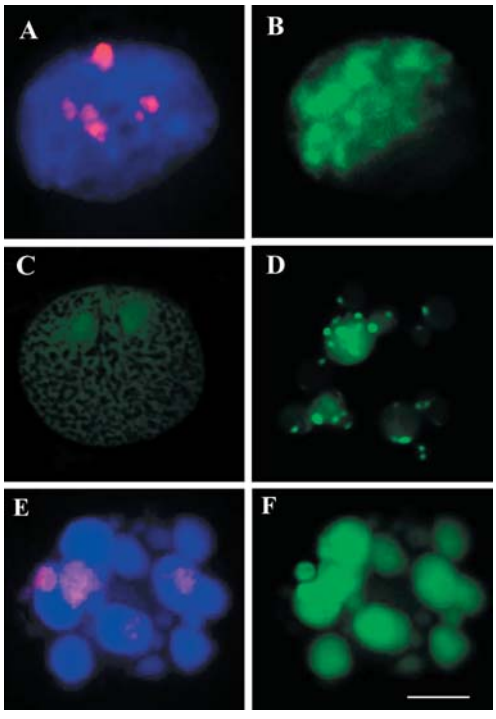

Figure 9. (*A*) Disassembly of chromosome 21 territories in the cell nucleus of an etoposide-treated K-562 cell. (*B*) The same nucleus (apoptotic bodies were still absent) was positive on the TUNEL test. (*C*) The nucleus of an intact cell was not stainable by the TUNEL technique. (*D*) Local intensive incorporation of fluorescein-dUTP was found in the apoptotic bodies of some K-562 nuclei after etoposide treatment. (*E*, *F*) Disassembly of territories of chromosome 11 (*E*) was observed in TUNEL-positive apoptotic nuclei (*F* is an example). Bar, 2 µm.

strated polyploidization induced by etoposide in K-562-VP16 cells (etoposide resistant) [36] and in mouse oocytes [37]. Etoposide and prolonged confluence are effective inducers of apoptosis [38], but since etoposide can also induce polyploidization in some cell types, prolonged confluence may also induce the simultaneous induction of apoptosis and polyploidization in parental K-562 cells.

FISH analysis and TUNEL test in apoptotic cells

As mentioned above, the architecture of chromosomal territories in apoptotic nuclei was studied using the FISH technique. In addition, an In Situ Cell Death Detection Kit (TUNEL test) was applied to distinguish apoptotic nuclei. In some interphase nuclei influenced by etoposide, the 3D-FISH procedure revealed the disassembly of chromosome 21 territories (fig. 9A). Coexistent TUNEL positivity was detected for the same nuclei (fig. 9B). Chromosomal territory segmentation seems to precede the formation of nuclear apoptotic bodies. Non-apoptotic cells were not stained by TUNEL techniques, which resulted in a low fluorescence signal (fig. 9C). In some 3D-fixed apoptotic bodies, local intensive incorporation of fluorescein-dUTP was observed (fig. 9D). These experiments confirmed that TUNEL-stained apoptotic nuclei fig. 9F) are characterized by variable disassembly of chromosomal territories (fig. 9E).

Discussion

Apoptosis, considered to be a cell suicide, can be found not only as a physiological process, but can also be observed in pathological disorders from cancer to autoimmune diseases [39–41]. It is a natural cell death found in animals as well as plants [42, 43]. A large variety of stimuli, both intracellular and extracellular, can initiate the cell death program [41, 44]. In the present experiments, apoptosis was induced in K-562 cells by the DNA-damaging agent etoposide and by prolonged confluence. The latter treatment is similar to the withdrawal of growth factors, as in the serum deprivation used in K-562 cells by Akiyama et al. [38]. Human erythroleukemia K-562 cells are characterized by their Bcr-Abl (Ph chromosome) positivity and by a substantially reduced p53 function. In our experiments, the withdrawal of growth factors probably inhibits the anti-apoptotic effect of the Bcr-Abl fusion protein, which was described in similar experiments by Cummings et al. [45].

Analyzing changes in the chromosomal architecture in apoptotic nuclei, we revealed differences in DNA fragmentation in tested cell lines. Different types of fragmen-

tation probably resulted in different accessibility of apoptotic chromatin to FISH staining of chromosomal territories. In particular, in K-562 cells with high-molecular-weight DNA fragmentation, we were successful in visualizing higher-order chromatin structures using the FISH technique. However, oligonucleosomal fragments of HL-60 cells undergoing prolonged confluence were not convenient for fluorescence hybridization. In addition, in our in situ chromatin experiments, we not only observed small chromosomal spots correlating to the size of the 50-kbp DNA probe, but we also found larger chromosomal segments (see fig. 7) that were probably bigger than those detectable using pulse field gel electrophoresis. On the other hand, the large segments may consist of 50- to 300-kbp fragments forming a compact part of the territory detected by FISH.

As mentioned above, two different types of DNA fragmentation reflected different accessibility of apoptotic DNA to FISH analysis. Apoptosis involves non-random DNA apoptotic digestion [9, 46, 47]: (i) DNA associated with the nuclear scaffold may be cleaved to large DNA fragments, (ii) histone H1 is removed and cleavage into both large and internucleosomal DNA fragments occurs, (iii) histone H1 is released at a later stage, and large DNA fragments precede internucleosomal DNA cleavage, (iv) only internucleosomal fragmentation is observed [9]. This type of DNA fragmentation (180–200 bp lengths) might be sustained by enhanced poly(ADP-ribosyl)ation of histone H1 which increases the susceptibility of chromatin to endonuclease activity [48]. Histone H1 release is required for 180- to 200-bp fragmentation [summarized in ref. 9], and therefore an absence of oligonucleosomal cleavage observed in tested apoptotic K-562 cells might be related to the inhibition of histone H1 disassembly from DNA. The variability in DNA degradation, cleavage at the linker region, and also DNA-histone interactions obviously play an important role in nuclear apoptotic destruction involving the changes in the architecture of chromosomal territories.

Our work is an attempt to contribute to knowledge of the apoptotic process from the perspective of higher-order chromatin organization. Interphase chromosomes occupy distinct territories and nuclear processes are governed by a specific compartmentalization [23, 26, 27, 49]. Our experiments indicate that chromosomal territories are variably disassembled into apoptotic nuclear segments and subsequently irregularly distributed into apoptotic bodies. Chromosomal territory segmentation seems to precede formation of apoptotic bodies, although we cannot exclude the further disassembly of chromosomal segments influenced by irregular formation of apoptotic bodies that differ in volume and number (compare figs 2, 3B). In our experiments, disassembly of chromosomal territories involving 50- to 300-kbp fragments was not observed at specific territorial sites as discussed by Earnshaw [8]. This suggestion is based on our observations revealing the possibility of segmentation at centromeric regions within chromosome 11 territories in K-562 apoptotic nuclei. Nevertheless, this finding can be explained either as a consequence of apoptosis or by polyploidization. Induction of polyploidization by etoposide was described by Melixetian et al. [36] and Mailhes et al. [37] in etoposide resistant K-562-VP16 cells and in mouse oocytes.

Variability in apoptotic body formation was also investigated. After exposure of cells to etoposide, we found approximately 17 apoptotic bodies per apoptotic cell, while after prolonged confluence, the number was only 7 on average. These differences in the formation of apoptotic bodies could be explained by various apoptotic events also described by other authors. Solovyan et al. [50] showed that the withdrawal of growth factors or etoposide treatment induced a distinct pattern of regulation of c-Fos, c-Jun, and p53 protein levels as well as differential changes in DNA-binding activity of AP-1 and NF-κB transcription factors playing an important role in the process of apoptosis. The late phase of apoptosis, induced by serum withdrawal, was associated with disintegration of nuclear DNA into both high-molecular-weight and oligonucleosomal DNA fragments, whereas etoposide induced the formation of large DNA fragments without oligonucleosomal DNA cleavage [50].

To eliminate the possibility of micronuclei formation [51, 52] after etoposide and prolonged confluence treatments, the presence of apoptotic nuclei was verified using the In Situ Cell Death Detection Kit (TUNEL test). From the literature we know that micronuclei can be observed in an irradiated cell population [53]. In our experiments, a DNA-damaging agent, etoposide, was used to induce apoptotic high-molecular-weight DNA fragmentation (fig. 1A) and formation of apoptotic bodies which was clearly verified using the TUNEL test (fig. 9) as well as with the aid of PI staining (see fig. 6). In addition, vital staining (annexin V versus PI and Hoechst 33342 versus PI) was also used to distinguish between the apoptotic, necrotic, and intact fraction of the tested etoposide-treated K-562 cell population. All measurements confirmed the presence of terminal stages of apoptosis and excluded secondary necrosis.

In summary, we showed that the appearance of apoptotic 50- to 300-kbp DNA fragmentation involves the variable disassembly of chromosomal territories into apoptotic bodies. Spatial and function-specific compartmentalization of chromosomal territories as well as the interchromosomal compartment [23–27] are degraded during the studied process. Apoptotic chromosomal segmentation seems to start before apoptotic body formation; however, chromosomal disassembly may proceed inside the apoptotic bodies.

Acknowledgements. This work was supported in part by the Academy of Sciences of the Czech Republic (grant No. S5004010, IAA 5004306 B5004102), grant MSM 143300002 (Ministry of Education of the Czech Republic) and by the Grant Agency of the Czech Republic (grant No. 301/01/0186). We would like to thank Dr. A. Kovařík for access to his laboratory to perform pulse field gel electrophoresis.

1 Kerr J. F. R., Wyllie A. H. and Currie A. R. (1972) Apoptosis: a basic biological phenomenon with wide-ranging implications in tissue kinetics. Br. J. Cancer. **26:** 239–257
2 Cohen J. J. (1994) Apoptosis: physiological cell death. J. Lab. Clin. Med. **124:** 761–765
3 Savill J., Dransfield I., Hogg N. and Haslett C. (1990) Vibronectin receptor-mediated phagocytosis of cells undergoing apoptosis. Nature **343:** 170–173
4 Rodolfo C. and Piacentini M. (2002) Does cytoskeleton 'Akt' in apoptosis? Cell Death Differ. **9:** 477–478
5 Thornberry N. A. and Lazebnik Y. (1998) Caspases: enemies within. Science **281:** 1312–1316
6 Faleiro L. and Lazebnik Y. (2000) Caspases disrupt the nuclear-cytoplasmic barrier. J. Cell Biol. **151**: 951–959
7 Hengartner M. O. (2000) The biochemistry of apoptosis. Nature **407:** 770–776
8 Earnshaw W. C. (1995) Nuclear changes in apoptosis. Curr. Opin. Cell Biol. **7:** 337–343
9 Bortner C. D., Oldenburg N. B. E. and Cidlowski J. A. (1995) The role of DNA fragmentation in apoptosis. Trends Cell Biol. **5:** 21–26
10 Martelli A. M., Bareggi R., Bortul R., Grill V., Narducci P. and Zweyer M. (1997) The nuclear matrix and apoptosis. Histochem. Cell. Biol. **108:** 1–10
11 Dusenbury C. E., Davis M. A., Lawrence T. S. and Maybaum T. S. (1991) Induction of megabase DNA fragments by 5-fluoredeoxyuridine in human colorectal tumor (HT29) cells. Mol. Pharmacol. **39:** 285–289
12 Brown D. G., Sun X. M. and Cohen G. M. (1993) Dexamethasone-induced apoptosis involves cleavage of DNA to large fragments prior to internucleosomal fragmentation. J. Biol. Chem. **268:** 3037–3039
13 Walker P. R., Smith C., Youdale T., Leblanc J., Whitfield J. F. and Sikorska M. (1991) Topoisomerase II-reactive chemotherapeutic drugs induce apoptosis in thymocytes. Cancer Res. **51:** 1078–1085
14 Sugimoto K., Yamada K., Egashira M., Yazaki Y., Hirai H., Kikuchi A. et al. (1998) Temporal and spatial distribution of DNA topoisomerase II alters during proliferation, differentiation, and apoptosis in HL-60 cells. Blood **91:** 1407–1417
15 Wyllie A. H. (1980) Glucocorticoid-induced thymocyte apoptosis is associated with endogenous endonuclease activation. Nature **284:** 555–556
16 Walker P. R., Kokileva L., LeBlanc J. and Sikorska M. (1993) Detection of the initial stages of DNA fragmentation in apoptosis. Biotechniques **15:** 1032–1040
17 Hale A. J., Smith C. A., Sutherland L. C., Stoneman V. E., Longthorne V. L., Culhane A. C. et al. (1996) Apoptosis: molecular regulation of cell death. Eur. J. Biochem. **236:** 1–26
18 Stewart B. W. (1994) Mechanisms of apoptosis: integration of genetic, biochemical, and cellular indicators. J. Natl. Cancer. Inst. **86:** 1286–1296
19 White E. (1996) Life, death, and the pursuit of apoptosis. Genes Develop. **10:** 1–15
20 Kluck R. M., Bossy-Wetzel E., Green D. R. and Newmeyer D. D. (1997) The release of cytochrome c from mitochondria: a primary site for Bcl-2 regulation of apoptosis. Science **275:** 1132–1136
21 Geske F. J. and Gerschenson L. E. (2001) The biology of apoptosis. Hum. Pathol. **32:** 1029–1038
22 Rich T., Allen R. L. and Wyllie H. (2000) Defying death after DNA damage. Nature **407:** 777–783
23 Cremer T., Kurz A., Zirbel R., Dietzel S., Rinke B., Schrock E. et al. (1993). Role of chromosome territories in the functional compartmentalisation of the cell nucleus. Cold Spring Harbor Symp. Quant. Biol. **58:** 777–792
24 Cremer T., Kreth G., Koester H., Fink R. H. A., Heintzmann R., Cremer M. et al. (2000) Chromosome domains, interchromatin domain compartment, and nuclear matrix: an integrated view of the functional nuclear architecture. Crit. Rev. Eukaryot. Gene Express. **12:** 179–212
25 Cremer T. and Cremer C. (2001) Chromosome domains, nuclear architecture and gene regulation in mammalian cells. Nat. Rev. Genet. **2:** 292–301
26 Verschure P. J., Kraan I. van der, Manders E. M. M. and Driel R. van (1999) Spatial relationship between transcription sites and chromosome domains. J. Cell Biol. **147:** 13–24
27 Spector D. L. (1993) Macromolecular domains within the cell nucleus. Annu. Rev. Cell Biol. **9:** 265–315
28 Chaly N. and Munro S. B. (1996) Centromeres reposition to the nuclear periphery during L6E9 myogenesis in vitro. Exp. Cell Res. **223:** 274–278
29 Bártová E., Kozubek S., Kozubek M., Jirsová P., Lukášová E., Skalníková M. et al. (2000) Nuclear topography of the *c-myc* gene in human leukemic cells. Gene **244:** 1–11
30 Bártová E., Kozubek S., Jirsová P., Kozubek M., Lukášová E., Skalníková M. et al. (2001) Higher-order chromatin structure of human granulocytes. Chromosoma **110:** 360–370
31 Bártová E., Kozubek S., Jirsová P., Kozubek M., Gajová H., Lukášová E. et al. (2002) Nuclear structure and gene activity in human differentiated cells. J. Struct. Biol. **139:** 76–89
32 Neves H., Ramos C., Silva M. G. da, Parreira A. and Parreira L. (1999) The nuclear topography of ABL, BCR, PML, and RAR alpha genes: evidence for gene proximity in specific phases of the cell cycle and stages of hematopoietic differentiation. Blood **93:** 1197–1207
33 Kozubek M., Kozubek S., Lukášová E., Marečková A., Bártová E., Skalníková M. et al. (1999) High-resolution cytometry of FISH dots in interphase cell nuclei. Cytometry **36:** 279–293
34 Bártová E., Špaňová A., Janáková L., Bobková M. and Rittich B. (1997) Apoptotic damage of DNA in human leukaemic HL-60 cells treated with C2-ceramide was detected after G1 blockade of the cell cycle. Physiol. Res. **46:** 155–160
35 Vondráček J., Štika J.V., Souček K., Minksová K., Bláha L., Hofmanová J. et al. (2001) Inhibitors of arachidonic acid metabolism potentiate tumour necrosis factor-alpha-induced apoptosis in HL-60 cells. Eur. J. Pharmacol. **424:** 1–11
36 Melixetian M. B., Beryozkina E.V., Pavlenko M. A. and Grinchuk T. M. (2000) Altered expression of DNA-topoisomerase II alpha is associated with increased rate of spontaneous polyploidization in etoposide resistant K562 cells. Leuk. Res. **24:** 831–837
37 Mailhes J. B., Marchetti F., Phillips G. L. Jr and Barnhill D. R. (1994) Preferential pericentric lesions and aneuploidy induced in mouse oocytes by the topoisomerase II inhibitor etoposide. Teratog. Carcinog. Mutagen. **14:** 39–51
38 Akiyama M., Yamada O., Kanda N., Akita S., Kawano T., Ohno T. et al. (2002) Telomerase overexpression in K-562 leukemia cells protects against apoptosis by serum deprivation and double-stranded DNA break inducing agents, but not against DNA synthesis inhibitors. Cancer Lett. **178:** 187–197
39 Williams G.T. (1991) Programmed cell death: apoptosis and oncogenesis. Cell **65:** 1097–1098
40 Williams G. T. and Smith C. A. (1993) Molecular regulation of apoptosis: genetic controls on cell death. Cell **74:** 777–779
41 Allen P. D., Bustin S. A., Macey M. G., Johnston D. H., Williams N. S. and Newland A. C. (1993). Programmed cell death (apoptosis) in immunity and haematological neoplasia. Br. J. Biomed. Sci. **50:** 135–149

42 O'Brien I. E. W., Murray B. G., Baguley B. C., Morris B. A. M. and Ferguson I. B. (1998) Major changes in chromatin condensation suggest the presence of an apoptotic pathway in plant cells. Exp. Cell Res. **241:** 46–54
43 Koukalová B., Kovařík A., Fajkus J. and Široký J. (1997) Chromatin fragmentation associated with apoptotic changes in tobacco cells exposed to cold stress. FEBS Lett. **414:** 289–292
44 Dini L., Coppola S., Ruzittu M. T. and Ghibelli L. (1996) Multiple pathways for apoptotic nuclear fragmentation. Exp. Cell Res. **223:** 340–347
45 Cummings M., Siitonen T., Higginbottom K., Newland A. C., and Allen P. D. (2002) p53-mediated downregulation of Chk1 abrogates the DNA damage-induced G2/M checkpoint in K-562 cells, resulting in increased apoptosis. Br. J. Haematol. **116:** 421–428
46 Oberhammer F., Wilson J. W., Dive C., Morris I. D., Hickmann J. A., Wakeling A. E. et al. (1993) Apoptotic death in epithelial cells: cleavage of DNA to 300 and/or 50kb fragments prior to or in the absence of intranucleosomal fragmentation. EMBO J. **12:** 3679–3684
47 Bicknell G. R. Snowden R. T. and Cohen G. M. (1994) Formation of high molecular mass DNA fragments is a marker of apoptosis in the human leukaemic cell line, U937. J. Cell Sci. **107:** 2483–2489
48 Noon Y. S., Kim J. W., Wang K. W., Kim Y. S., Choi K. H. and Joe C. O. (1996) Poly (ADP-ribosyl)ation of histone H1 correlates with internucleosomal DNA fragmentation during apoptosis. J. Biol. Chem. **271:** 9129–9134
49 Kurz A., Lampel S., Nickolenko J. E., Bradl J., Benner A., Zirbel R. M. et al. (1996) Active and inactive genes localise preferentially in the periphery of chromosome domains. J. Cell Biol. **135:** 1195–1205
50 Solovyan V., Bezvenyuk Z., Huotari V., Tapiola T., Suuronen T. and Salminen A. (1998) Distinct mode of apoptosis induced by genotoxic agent etoposide and serum withdrawal in neuroblastoma cells. Brain Res. Mol. Brain Res. **62:** 43–55
51 Fenech M. and Morley A. A. (1985) Measurements of micronuclei in lymphocytes. Mutat. Res. **147:** 29–36
52 Savage J. R. K. (1989) Acentric chromosomal fragments and micronuclei: the time-displacement factor. Mutat. Res. **207:** 171–173
53 Fenech M. and Morley A. A. (1986) Cytokinesis-block micronucleus method in human lymphocytes: effect of in vivo ageing and low-dose X-irradiation. Mutat. Res. **161:** 193–198